Photon-counting microscopy of terahertz radiation

Kenji Ikushima,[a] Yasuhiro Yoshimura, Takuma Hasegawa, and Susumu Komiyama
Department of Basic Science, University of Tokyo, Komaba, Meguro-ku, Tokyo 153-8902, Japan

Takeji Ueda
SORST, Japan Science and Technology Corporation (JST), Kawaguchi, Saitama 332-0012, Japan

Kazuhiko Hirakawa
Institute of Industrial Science, University of Tokyo, Komaba, Meguro-ku, Tokyo 153-8505, Japan

(Received 10 January 2006; accepted 27 February 2006; published online 13 April 2006)

Photon-counting imaging of terahertz radiation is demonstrated with a spatial resolution of 50 μm for a free-space wavelength of 132 μm by incorporating a quantum-dot single photon detector into a scanning confocal optical system. Terahertz radiation of 10^{-19}–10^{-16} W or 10^{2}–10^{5} photons/s is imaged. Applying the microscope to the study of semiconductor quantum Hall devices, a threshold behavior of the cyclotron emission is found and the mechanism is discussed. © *2006 American Institute of Physics*. [DOI: 10.1063/1.2194473]

In the visible/near-infrared microscopy, the photon-counting method is indispensable for detecting extremely weak radiation.[1] The method, however, has been inaccessible in terahertz region (1 THz$\approx$33 cm^{-1} or 4 meV). This is because the photon energies are more than 100 times smaller and catching individual photons is difficult. Recently, however, the situation is beginning to change. That is, superconducting transition-edge sensors are expanding the spectral range of photon counting towards the midinfrared region.[2] Furthermore, by using semiconductor quantum dots (QDs), photon detectors have been developed in the far longer-wavelength terahertz region (wavelengths λ of 175–210 and 600 μm).[3,4] In the latter detectors, a QD serves as a key element in a single electron transistor (SET). Being absorbed by the QD, a terahertz photon induces an electrical polarization of the QD, which is in turn, detected by the SET with an extraordinarily high sensitivity. Here we report the application of the QD photon detector in true measurements. We improve the detection scheme so as to achieve faster detection speed at elevated temperatures, and design a scanning confocal optical microscope, in which the QD photon detector is incorporated. By applying the microscope system to the study of quantum Hall (QH) electron systems, we reveal features of the dynamics of nonequilibrium electron generation.

We first describe the QH electron systems to be studied. In a two-dimensional electron system (2DES) in a strong magnetic field (B), the kinetic energy splits into discrete Landau levels separated by the cyclotron energy $\hbar\omega_c$ ($\hbar=h/2\pi$ with Planck's constant h). In the QH state, terahertz emission is expected to be strictly absent because the electron system is deemed to be in the dissipationless state with zero longitudinal resistance. However, if, for some mechanisms, nonequilibrium electrons (holes) are generated in Landau levels above (below) the Fermi level, terahertz photons with the cyclotron energy are emitted through radiative recombination. Imaging the cyclotron emission (CE) is therefore a powerful tool to probe local density profile of the excited nonequilibrium electrons. By using simple terahertz microscopes[5,6] with an integration-type QH detectors,[7,8] earlier studies have found generation of nonequilibrium electrons on electron entry and exit corners of Hall bars[5] or have visualized unequally populated edge states.[9] Owing to the lack of the detector sensitivity, however, an array of more than 10 000 Hall bars was needed to obtain detectable signals.[5] Or large source-drain bias voltages V_{sd} far beyond $\hbar\omega_c/e$ (e is the unit charge) was needed.[5,9] In order to achieve deeper understanding of the mechanism of nonequilibrium electron generation, measurements at $V_{sd}\sim\hbar\omega_c/e$ are highly desirable, which require a photon-level sensitivity or a better sensitivity by a factor more than 1000.

The QD detector, utilizing the cyclotron resonance of electrons in the QD, is fabricated in a GaAs/AlGaAs heterojunction of an electron density $n_{2D}=3.2\times10^{15}$ m^{-2} and a mobility $\mu=80$ m^2/V s [Fig. 1(a)] via a standard electron beam lithography.[3] In the first demonstration experiment,[3] a ^{3}He–^{4}He dilution refrigerator was used to achieve ultralow temperatures ($<$0.1 K), at which the detection is feasible because of long lifetimes of the excited polarization ($>$1 ms). To construct a scanning terahertz microscope here, we need to use a more compact ^{3}He refrigerator, the base temperature of which is limited to 0.3 K. The lifetime of the photoexcited polarization state is thereby reduced by a factor of about 10^{-2}, requiring a faster detection speed up to an order of 10 μs. For this sake, we operate the SET in a constant voltage mode and detect the current through a voltage drop across a series resistance (40 kΩ) to the SET placed at a low temperature. Also by minimizing the stray capacitance of the wiring, we improve the operation speed to 20 μs as shown in the top curve of Fig. 1(b). The faster detection speed leads also to the expansion of the linear dynamic range beyond 30 dB. In the actual measurements at 0.3 K, the dark switching of the SET limits the sensitivity, which is found to be about 0.1 count/s at $\lambda=132$ μm. The quantum efficiency, depending on the coupling between the designed planar antenna and the QD, is roughly about 10% when the incident light comes from a high dielectric constant material of GaAs. This corresponds to the incidence of about 1 photon/s, or 10^{-21} W, on the detector, and is about 1000 times more sensitive than the level of present astronomy.[10] A spectral resolution of $\Delta\lambda/\lambda<0.05$ is obtained by the narrow-band resonance absorption of the detector, where the wavelength of

[a]Electronic mail: ikushima@thz.c.u-tokyo.ac.jp

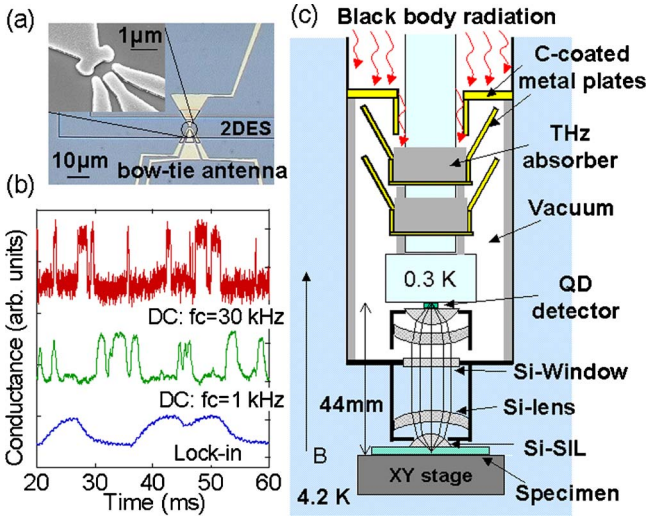

FIG. 1. (Color online) (a) Optical micrograph of the QD photon detector fabricated in a GaAs/AlGaAs. Metal gates define the QD (0.7×0.7 μm^2) when negatively biased as shown in the inset (a scanning electron micrograph) and serve also as a bow-tie antenna that couples incident terahertz waves to the QD. (b) Real time traces of the photon-counting signals (conductance switches) at $T=0.3$ K. Three curves display results obtained in different schemes. A lock-in modulation technique yields a response time constant of $\tau_c=1.25$ ms (bottom). A faster response with $\tau_c=60$ and 20 μs (middle and top) are obtained in a constant voltage mode, where f_c denotes the cutoff frequency of the low-pass filters used. (c) Schematic diagram of the photon-counting microscope.

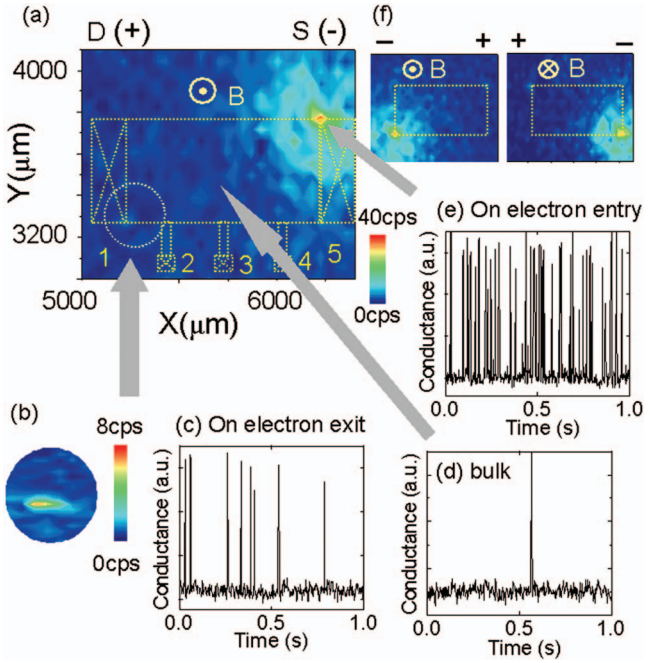

FIG. 2. (Color) (a) Rates of terahertz photon counting, detected in the $\nu=2.00$ QH state at 1.2 μA, are color mapped (red, 40 cps; blue, 0 cps). The terahertz photons are of $\hbar\omega_c=9.43$ meV ($\omega_c=2\pi\times2.28$ THz) or the wavelength of 132 μm. (b) The emission on the drain corner is made visible by enhancing the sensitivity on the expanded XY scale by a factor of 1.5. [(c)–(e)] SET conductance switches showing the events of photon arrival to the detector from different positions: the drain corner (c), the bulk region (d), and the source corner (e). (f) Terahertz photon-counting images with the opposite polarities of the current and the magnetic field.

the maximum sensitivity is magnetically tunable over $\lambda=120-170$ μm.

Figure 1(c) shows the scanning confocal optical system developed. The QD detector is cooled down to $T=0.3$ K while the specimen (QH device) at a higher temperature (4.2 K) is separated by vacuum at a distance of about 44 mm from the detector.[11] Both the objective lens system and the detector-lens system are a coupled silicon hyperhemisphere lenses designed to be aplanatic. The objective lens, serving as a solid immersion lens (SIL), is moderately pushed to the backside of the QH device by using a CuBe spring. Terahertz waves from the device at the focal point of the SIL are transmitted through a silicon window and refocused on the detector. By moving the QH device with a piezo-driven XY stage, the focal point scans the whole area of the device. Two-dimensional pictures of terahertz radiation on attowatt levels or 10^2-10^5 photons/s are thus obtained. Owing to the aplanatic lens system, a resolution of 50 μm is attained for a free-space wavelength of 132 μm. Multiple carbon-coated (C-coated) metal plates shield the blackbody radiation straying from higher-temperature environments onto the detector through the vacuum space.

Figures 2(a) and 2(b) show photon-counting images of the CE from the QH bar at the filling factor of $\nu=2$ ($B=5.62$ T, $\hbar\omega_c=9.43$ meV) with a current at 1.2 μA (the source-drain bias of $V_{15}=15.5$ mV). Though not shown here, the perfect QH state is realized in the 2DES in this condition, where the longitudinal resistance as well as the excess contact resistance are indiscernibly small and the Hall resistance is quantized. Nevertheless, distinct events of photon emission are noted as shown by the SET current switching in Figs. 2(c)–2(e). The rate of counting is color coded to yield the images of Figs. 2(a) and 2(b). The broken line illustrates a 1-mm-long and 0.5-mm-wide Hall bar studied, fabricated on a GaAs/AlGaAs heterojunction ($n_s=2.7\times10^{15}$ m^{-2} and $\mu=27$ m^2/V s). Two bright spots are recognized on the diagonally opposite two corners of the 2DES layer at the interfaces to with current contacts. The brighter spot is on the electron entry corner (the source contact) and the less bright spot is on the exit corner (the drain contact). Emission is absent in the interior region of the Hall bar. The imaging pictures taken in the opposite polarities of current and magnetic field [Fig. 2(f)] evidence that the feature is intrinsic to the QH device. Since the sensitivity is practically unlimited, we are able to track the emission down to submicroampere levels as shown in Fig. 3(a). A distinct threshold is found for the emission on source corner at $V_{15}\approx\hbar\omega_c/2e=4.72$ mV (0.365 μA). The threshold is different for the drain corner, being at $V_{15}\approx\hbar\omega_c/e=9.43$ mV (0.730 μA). These findings are interpreted as follows. On the entry corner, nonequilibrium electrons can be generated via electron tunneling through the potential barrier formed at the interface with the contact.[5] Since the electrochemical potential of the source lines up with the empty $N=1$ lowest Landau level, this tunneling is permitted when eV_{15} reaches $\hbar\omega_c/2$ [Fig. 3(b)]. On the exit corner, however, tunneling processes take place via inter-Landau-level transitions at a potential fall, which leads to a threshold of $eV_{15}\sim\hbar\omega_c$ [Fig. 3(c)].

We have demonstrated the powerfulness of the photon-counting terahertz microscopy for the study of QH electron systems. Possible applications, however, should be broader. QD detectors without the use of magnetic field[4] can be applied for the objects in zero magnetic fields. A dramatic improvement of the spatial resolution can be expected by introducing the near-filed technique with micro metal-tip antennas.[12] Given a microscope of such higher resolutions with low background level of blackbody radiation, the appli-

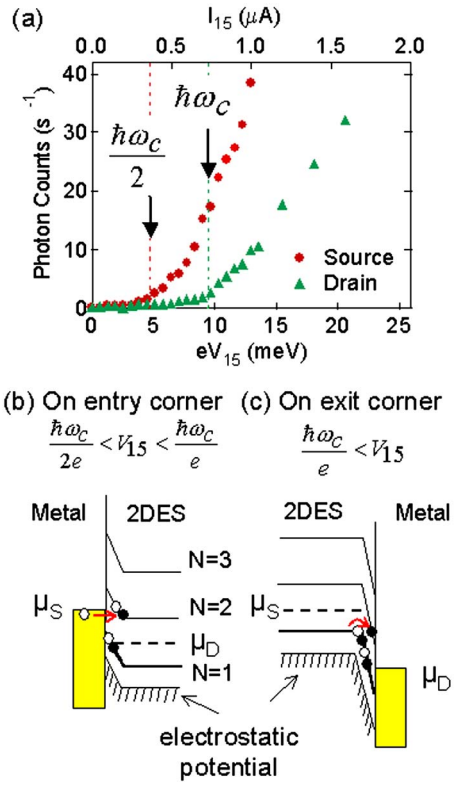

FIG. 3. (Color online) (a) Photon-count rate vs the source-drain bias voltage (bottom axis). The values of current are marked on the top axis. The circles and the triangles represent the data on the source and the drain corners, respectively. [(b) and (c)] Schematic representations of the energy profile on the electron entry corner at $\hbar\omega_c/2e < V_{15} < \hbar\omega_c/e$ and on the exit corner at $\hbar\omega_c/e < V_{15}$.

cation may be expanded to studies of higher-temperature objects.

This work was supported by Solution Oriented Research for Science and Technology (SORST) from Japan Science and Technology Corporation (JST) and by Grant-in-Aid for Specially Promoted Research from the Japanese Ministry of Education, Culture, Sports, Science and Technology.

[1]For example, with avalanche silicon diodes, near-infrared photon counting is applied to single molecule detection via fluorescence; See *Single Molecule Detection in Solution: Methods and Applications*, 1st ed., edited by C. Zander, J. Enderlein, and R. A. Keller (Wiley-VCH, Berlin, 2002), p. 323.
[2]A. Lipatov, O. Okunev, K. Smirnov, G. Chulkova, A. Korneev, P. Kouminov, G. Gol'tsman, J. Zhang, W. Slysz, A. Verevkin, and R. Sobolewski, Supercond. Sci. Technol. **15**, 1689 (2002).
[3]S. Komiyama, O. Astafiev, V. Antonov, T. Kutsuwa, and H. Hirai, Nature (London) **403**, 405 (2000).
[4]O. Astafiev, S. Komiyama, T. Kutsuwa, V. Antonov, Y. Kawaguchi, and K. Hirakawa, Appl. Phys. Lett. **80**, 4250 (2002).
[5]Y. Kawano, Y. Hisanaga, and S. Komiyama, Phys. Rev. B **59**, 12537 (1999).
[6]K. Ikushima, H. Sakuma, and S. Komiyama, Rev. Sci. Instrum. **74**, 4209 (2003).
[7]Y. Kawano, Y. Hisanaga, H. Takenouchi, and S. Komiyama, J. Appl. Phys. **89**, 4037 (2001).
[8]B. A. Andreev, I. V. Erofeeva, V. I. Gavrilenko, A. L. Korotkov, A. N. Yablonskiy, O. Astafiev, Y. Kawano, and S. Komiyama, Semicond. Sci. Technol. **16**, 300 (2001).
[9]K. Ikushima, H. Sakuma, S. Komiyama, and K. Hirakawa, Phys. Rev. Lett. **93**, 146804 (2004).
[10]P. H. Siegel, IEEE Trans. Microwave Theory Tech. **50**, 910 (2002).
[11]The QD detector is based on the plasma-coupled resonance, the frequency of which is by about 4% higher than the cyclotron resonance frequency in the QH device. To match these frequencies, the QH device is placed near the center of the solenoid while the QD detector is offset from the center.
[12]Hou-Tong Chen, R. Kersting, and G. C. Cho, Appl. Phys. Lett. **83**, 3009 (2003).